# Reduction of CaO and MgO Slag Components by Al in Liquid Fe

HAOYUAN MU, TONGSHENG ZHANG, RICHARD J. FRUEHAN, and BRYAN A. WEBLER

This study documents laboratory-scale observations of reactions between Fe-Al alloys (0.1 to 2 wt pct Al) with slags and refractories. Al in steels is known to reduce oxide components in slag and refractory. With continued development of Al-containing Advanced High-Strength Steel (AHSS) grade, the effects of higher Al must be examined because reduction of components such as CaO and MgO could lead to uncontrolled modification of non-metallic inclusions. This may lead to castability or in-service performance problems. In this work, Fe-Al alloys and CaO-MgO-$Al_2O_3$ slags were melted in an MgO crucible and samples were taken at various times up to 60 minutes. Inclusions from these samples were characterized using an automated scanning electron microscope equipped with energy dispersive x-ray analysis (SEM/EDS). Initially $Al_2O_3$ inclusions were modified to $MgAl_2O_4$, then MgO, then MgO + CaO-$Al_2O_3$-MgO liquid inclusions. Modification of the inclusions was faster at higher Al levels. Very little Ca modification was observed except at 2 wt pct Al level. The thermodynamic feasibility of inclusion modification and some of the mass transfer considerations that may have led to the differences in the Mg and Ca modification behavior were discussed.

https://doi.org/10.1007/s11663-018-1294-8


## I. INTRODUCTION

RECENT development of new Advanced High-Strength Steel (AHSS) grades has resulted in higher levels of the alloying elements Si, Mn, Al, and Cr than traditional low-C Al-killed grades.[1–3] Particularly important is Al, as increased dissolved Al content can reduce MgO, CaO, and other oxides that comprise ladle slags and refractories at liquid steel refining temperatures. Reduction of these slag components leads to Ca or Mg transfer to inclusions in the steel and uncontrolled changes to inclusions, leading to castability or performance problems.

HAOYUAN MU is with the Advanced Refractories Division of Vesuvius, Bettsville, OH, 44815. TONGSHENG ZHANG is with the Center for Iron and Steelmaking Research, Carnegie Mellon University, Pittsburgh, PA, 15213 and with the School of Metallurgy and Environment, Central South University, Changsha, China and also with the National Center for International Research of Clean Metallurgy, Central South University. RICHARD J. FRUEHAN is with the Center for Iron and Steelmaking Research, Carnegie Mellon University. BRYAN A. WEBLER is with the Center for Iron and Steelmaking Research, Carnegie Mellon University and also with the Materials Science and Engineering Department, Carnegie Mellon University. Contact e-mail: webler@cmu.edu
Manuscript submitted September 20, 2017.
Article published online May 21, 2018.

Several previous studies have investigated the reduction of slag and refractory components in Al-killed (approx. 0.03 wt pct Al) steels. Spinel ($MgOAl_2O_3$) formation due to MgO reduction has been the most extensively studied, often in stainless steels since spinel inclusions are detrimental to production processes and final properties.[4–11] Mass transfer of Mg in liquid steel has been shown to be the rate determining step in the MgO reduction and spinel formation processes.[10–13] Researchers have investigated the thermodynamics of MgO reduction from slags and spinel inclusion formation and suggested to optimize the time of Al additions for deoxidation and to minimize MgO activity in slags.[4,9] If the steel is Ca treated, the spinel inclusions can be modified to CaO-MgO-$Al_2O_3$, where the MgO in the inclusions is reduced by the added Ca.[7,14–17] Metallic Mg additions can likewise modify CaO-$Al_2O_3$ inclusions to CaO-MgO-$Al_2O_3$ with possible CaO-$Al_2O_3$ cores.[18]

Even without Ca treatment, previous work has suggested that sufficient Ca can be transferred from the slag and modify spinel inclusions to liquid calcium aluminates when slag was reduced by metallic Al additions.[8,9] Liquid calcium aluminate, usually formed at the interfaces of original inclusion and metal, has been shown to be stable at 1873 K (1600 °C) even though dissolved Ca content in liquid steel is very low.[7–9,14–17] However, reduction of CaO has not been as extensively studied as has reduction of MgO. Some of

the challenges in quantifying the reduction of CaO is due to the large variability in the thermodynamics of dissolved Ca in liquid iron.[19] It is possible, however, that some inferences about the dissolved Ca behavior can be made by studying the changes to the non-metallic inclusion populations.

Simultaneous CaO and MgO reduction by dissolved Al in steels has already been reported to result in unintended changes to inclusion chemistries in industrial production of AHSS.[20–23] The industrial observations of Ca modification were usually correlated with CaO-rich slag, long ladle process times, and heavy stirring in the ladle.[20] These observations would be consistent with a hypothesis that mass transfer of Ca in the liquid steel controlled the rate of inclusion modification because the industrial conditions under which Ca transfer was observed corresponded to conditions where there would be the highest driving force, longest reaction time, and highest mass transfer coefficient. Others have noted that high Al level (3 to 6 wt pct) led to a change of slag chemistry and viscosity, which might result in a slowdown of mass transfer from slag to steel.[23]

In general, inclusion chemistry changes occur because the inclusions in the steel are not in chemical equilibrium with the slag and the refractory. For example, when CaO and MgO-saturated slags cover an Al-killed steel, the initially $Al_2O_3$ inclusions should eventually transform to inclusions saturated with CaO and MgO if they do not first float and separate to the slag. The transformation must be accomplished by mass transfer of elements and inclusion chemistries evolve during time scales equivalent to that of ladle processing (approx. 30 to 60 minutes).

Mass transfer at interfaces has been modeled with two different approaches. The first is the two-film theory of mass transfer which considers the coupled chemical reactions and fluxes of species at the interface.[11–13,24,25] The second approach assumes equilibrium over a finite volume at the surface and uses FactSage for equilibrium calculations.[26–29] In these studies, the mass transfer in the metal at the slag/metal interface was considered to be the rate-controlling process for inclusion modification.

This paper documents laboratory-scale experiments on the effect of Al level on the simultaneous reduction behavior of both CaO and MgO. Fe-Al melts with Al contents up to 2 wt pct were reacted with CaO, MgO, $Al_2O_3$ slags (CaO and MgO saturated) for up to 60 minutes. An induction furnace with a graphite susceptor was used, so the only stirring was due to natural convection. The resulting changes to the initially $Al_2O_3$ non-metallic inclusions were measured over time using automated inclusion analysis methods. Although the mass transfer coefficients will be different for a gas-stirred ladle, the results showed higher Al levels can lead to large changes in non-metallic inclusion composition.

## II. EXPERIMENTAL METHODS

### A. *Materials*

In each experiment, approximately 500 g of an Fe-Al melt was prepared by mixing and pre-melting two master alloys. Analysis of the master alloy chemistry and inclusion contents is given in Table I. These alloys were mixed to create starting alloys of 0.1, 0.5, 1, and 2 wt pct Al. Initial inclusions were analyzed using methods described in Section II–D. Inclusions were predominately $Al_2O_3$ in both master alloys. The average inclusion diameter was in the range from 1 to 1.5 $\mu$m.

To create the slags, pure CaO powders were calcined at 1173 K (900 °C) for 12 hours. These powders were mixed with pure $Al_2O_3$ in the ratio of $CaO/Al_2O_3 = 1$ (by mass), then pre-melted in a graphite crucible and subsequently decarburized in air at 1273 K (1000 °C). Pure CaO and MgO powders were later added to make the slag saturated with respect to both CaO and MgO. The saturated slag chemistry was based on a FactSage calculation for a temperature of 1873 K (1600 °C), and examination of literature data.[30,31] The double-saturated slag chemistry used was 51 wt pct CaO-39 wt pct $Al_2O_3$-10 wt pct MgO.

High-purity (99 pct) and dense MgO crucibles (outer diameter 62 mm, inner diameter 49 mm, and height 150 mm) were produced by slip casting and supplied by Tateho Ozark. MgO crucibles were selected to minimize reaction with the MgO-saturated slag and because MgO-containing refractory materials can be used during industrial operations.

### B. *Setup*

A 10 kW Ameritherm induction furnace was used for the slag–metal reaction. Figure 1 shows a schematic of the experimental setup. The furnace was set vertically for sampling and slag addition under high temperatures. The metal and slag were contained in an MgO crucible, which was in turn surrounded by a graphite crucible. The graphite crucible acted as a susceptor to heat and melt both slag and metal samples, in addition to serving as a protective outer crucible. The reaction chamber that contained the crucibles was a fused quartz tube with $Al_2O_3$ insulating paper wrapped inside. The guidance tube was designed for adding slag and taking samples. The temperature was measured by a B-type thermocouple from the top. High-purity argon (99.9999 pct) was firstly passed over heated Mg chips in an oxygen getter furnace and then introduced into the reaction chamber at a flow rate of 300 mL/min.

### C. *Procedure*

A total of 500 g of Fe-Al alloy was used for each experiment. The MgO crucibles used had inner diameters of 5.1 cm and were 14.0 cm tall. This metal charge was heated in the induction furnace at 5 K/min to the reaction temperature, usually 1873 K (1600 °C). The system was then held for 30 minutes before taking the initial metal sample. A quartz tube with 3 mm inner diameter was inserted through the guidance tube and a pipette was used to siphon liquid alloy into the sampling quartz tube. The tube was then quenched in cold water and a pin metal sample was formed inside. After taking the initial sample, 75 g slag was added onto the surface of liquid alloy also through guidance tube. Subsequent samples were taken at the time points as shown in

Table I. Master Alloys Mixed to Make Melts with Al Contents 0.1, 0.5, 1, 2 Wt Pct

| | Composition (in ppm Unless Otherwise Stated) | | | | Inclusions | | | |
|---|---|---|---|---|---|---|---|---|
| No. | C | Al (Weight Percent) | S | Ca | Majority Type | Average Diameter ($\mu$m) | Number Density (#/mm$^2$) | Area Density ($\mu$m$^2$/mm$^2$) |
| Alloy 1 | 4 | 0.019 | 10 | < 1 | $Al_2O_3$ | 1.01 | 56 | 65 |
| Alloy 2 | 8 | 2.207 | 10 | < 10 | $Al_2O_3$ | 1.49 | 28 | 115 |

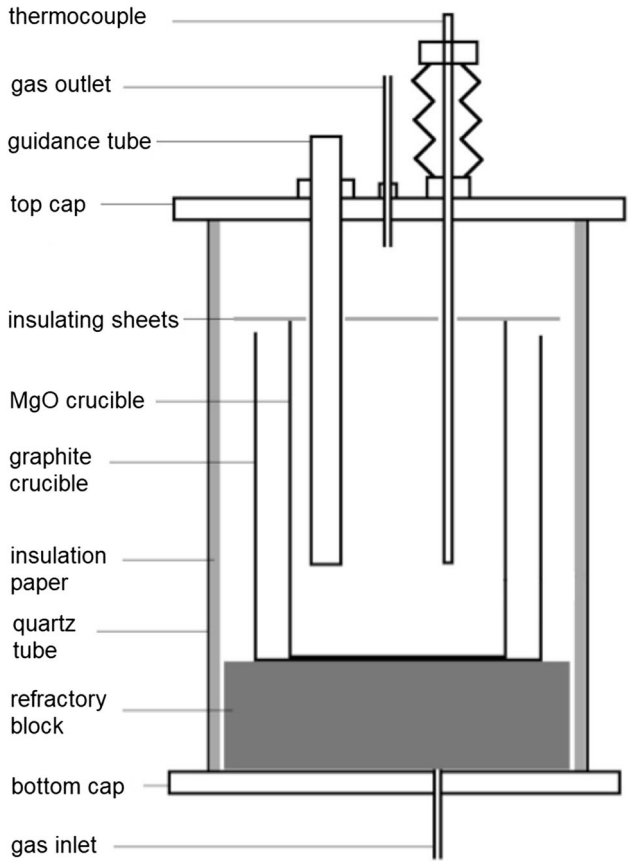


Fig. 1—Schematic of the induction furnace setup.

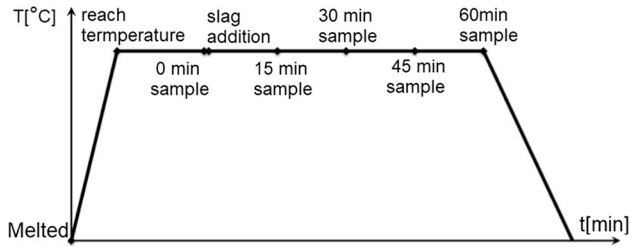


Fig. 2—The temperature–time profile for sampling and slag addition.

Figure 2. This procedure was adopted to establish an accurate start time for the metal–slag reaction. A temperature transient was observed on slag addition but the duration was short, approximately 5 minutes. Two experiments were performed at a target reaction temperature of 1973 K (1700 °C). Stabilizing this temperature was difficult and while the experiment proceeded at a temperature above the standard reaction temperature of 1873 K (1600 °C), the actual temperature during these experiments was variable.

### D. *Material Characterization*

Automated inclusion analysis was performed on an FEI/ASPEX Explorer SEM. Samples were metallographically prepared and analyzed by a SEM under 10 kV accelerating voltage.[32] Inclusions larger than 0.5 $\mu$m were analyzed. The collected data were manually filtered to remove pores and surface contamination. In most samples, 150 to 500 inclusions were examined. However, samples taken after long hold times had low inclusion densities and in these samples, approximately 50 inclusions were measured.

Total Al, Ca, and Mg contents in this study for select experiments were measured by inductively coupled plasma mass spectroscopy (ICP-MS) and reported to the nearest 10 ppm. Total oxygen content was quantified by LECO N/O. Slag composition was measured at the end of select experiments by X-ray fluorescence (XRF) spectroscopy with a detection limit about 1000 ppm.

All equilibrium calculations in this study were performed with FactSage version 7.1[33] using the FactPS (pure substances), FToxid (oxide solution), and FTmisc (liquid metal solution) databases.

## III. EXPERIMENTAL RESULTS

### A. *Summary of Experiments*

As described in Table II, eight experiments were designed and conducted to study the effects of Al content and reaction temperature on Mg and Ca transfer. Experiments in this table are named in the form of "[Al content]_[slag composition]." Al contents were always expressed in weight percent. The slag composition labels were CAM, NONE, and CA represent CaO-$Al_2O_3$-MgO (double-saturated) slag, no slag, and CaO-$Al_2O_3$ slag (initially CaO-saturated), respectively. Experiments with "(+T)" were conducted at a temperature above 1873 K (1600 °C), but this temperature was not necessarily constant. All experiments were conducted in an MgO crucible.

Table II. Experiments Designed to Study the Effects of Slag Composition, Al Content, and Reaction Temperature

| Experiment | Reaction Temperature | Slag Composition | Designed Al Content |
|---|---|---|---|
| 2AL_CAM | 1873 K (1600 °C) | CaO: 51 wt pct | 2 wt pct |
| 1AL_CAM | | $Al_2O_3$: 39 wt pct | 1 wt pct |
| 0.5AL_CAM | | MgO: 10 wt pct | 0.5 wt pct |
| 0.1AL_CAM | | | 0.1 wt pct |
| 2AL_CAM(+T) | > 1873 K (1600 °C) | | 2 wt pct |
| 1AL_CAM(+T) | | | 1 wt pct |
| 2AL_NONE | 1873K (1600 °C) | none | 2 wt pct |
| 2AL_CA | | CaO: 57 wt pct | 2 wt pct |
| | | $Al_2O_3$: 43 wt pct | |

### B. *Metal Composition*

The measurements of total Al and total Mg for selected samples are given in Figure 3. In this figure, time zero is the time of slag addition.

The decreasing trend in Al was caused in part by reduction of Mg and Ca but more so by reoxidation that occurred due to air introduced during slag addition and sampling. This was most apparent in the 0.5AL_CAM experiment, which exhibited large Al fade. Total oxygen measurements in this sample were 60 ppm (average over the experiment) and the inclusion chemistries (see Section III–D) showed evidence of reoxidation. Total oxygen in other experiments averaged 20 ppm (average of several experiments over time). Other evidence of reoxidation in certain samples will be shown in Section III–D.

Despite reoxidation effects, certain trends could be identified from chemistry measurements. For the experiments with the CAM slag, total Mg levels increased with increasing Al content. The 2AL_NONE samples exhibited less Al fade and lower Mg levels. The 2Al_CA samples exhibited similar total Mg levels to the 2AL_CAM samples. Finally, increasing the temperature led to much higher total Mg levels.

Measurements of total Ca were attempted but almost all results were reported below 10 ppm, the detectable threshold for the instrument used. The exception to this was the experiment 2Al_CAM(+T), where total Ca was 20 ppm after 30 minutes reaction.

### C. *Slag Composition*

Slag composition analysis was conducted on the slags after 60 minutes reaction time in three experiments with 2 wt pct Al addition. The designed slag composition before experiments and the analyzed slag composition after experiments are listed in Table III. Initial compositions were calculated based on mixing of oxide powders. Final compositions were measured by XRF. In experiments where the slag initially contained MgO, the weight percentage of MgO and $Al_2O_3$ slightly increased while the weight percentage of CaO in slags decreased. In the CA experiment, the MgO content increased from 0 to 10.7 wt pct with a corresponding decrease in CaO.

### D. *Evolution of Inclusion Chemistry*

The measured inclusion chemistry changes from each experiment are shown in this section. Inclusion chemistries are represented by plotting the inclusion cation mole fraction on Ca-Mg-Al ternary diagrams. The size of each triangle symbol on the diagram was proportional to area fraction of inclusions of approximately that composition.

The experiment 2AL_NONE was conducted to examine inclusion chemistry evolution after only metal/crucible reaction. The evolution of inclusion chemistry with time for this experiment is shown in Figure 4.

Figure 5 presents the evolution of inclusion chemistries in Experiments 2AL_CAM to 0.1AL_CAM, which were performed to study the reactions between an alloy containing 2 wt pct to 0.1 wt pct Al with a dense MgO crucible and CaO, MgO double-saturated slag.

Spinels were the typical inclusion types before slag addition. Inclusion Mg and Ca content increased with time and Al content. Measurable Mg modification appeared to occur first and transformation from spinel to MgO inclusions was observed for all Al levels. The effects of reoxidation during slag addition or sampling were evident in the following samples: 0 minute 2AL_CAM, 60 minutes 2AL_CAM, 30 minutes 1AL_CAM, 15 minutes 0.5AL_CAM, and 15 minutes 0.1AL_CAM. The effect of reoxidation is further discussed below. Several Ca-containing inclusions in experiment 2AL_CAM were examined *via* manual SEM/EDS. Two examples are shown in Figure 6.

These inclusions had MgO cores and a calcium aluminate shell that contained some Mg. The Ca/Al ratio in Al-Ca-Mg-containing inclusions was slightly less than unity, indicating the formation of liquid or partially liquid inclusions. This was supported by the globular outlines of such Al-Ca-Mg-containing inclusions.

The inclusion chemistry changes for experiment 2AL_CA are shown in Figure 7. This experiment was conducted to examine if eliminating MgO from the initial slag would affect inclusion chemistry evolution. The results were similar to those reported in Figure 5(a), but the inclusion Mg content was lower.

Finally, the inclusion chemistry changes for experiments 2Al_CAM(+T) and 1Al_CAM(+T) are shown

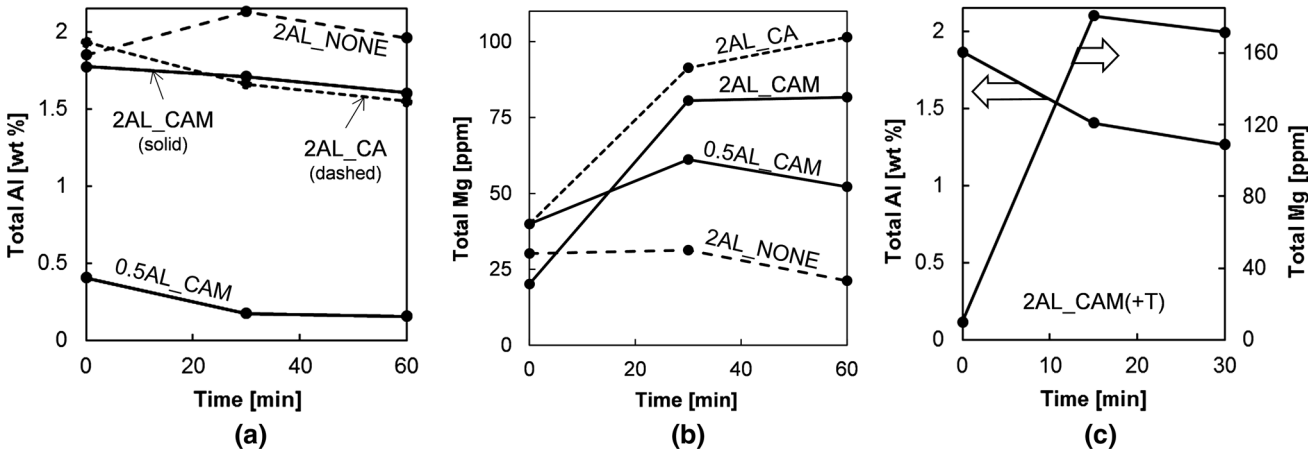


Fig. 3—Sample chemistry changes with time for (*a*) total Al contents in 1873 K (1600 °C) experiments, (*b*) total Mg contents in 1873 K (1600 °C) experiments, and (*c*) total Al and total Mg contents for experiment 2AL_CAM(+T) [note the change in *y*-axis for Total Mg in (c)].

**Table III. Slag Compositions for Experiments "2Al_CAM," "2Al_CA," and "2Al_CAM(+T)"**

| Experiment | $Al_2O_3$ (Weight Percent) | CaO (Weight Percent) | MgO (Weight Percent) |
|---|---|---|---|
| 2Al_CAM Initial | 39 | 51 | 10 |
| 2Al_CAM Final | 42.0 | 46.8 | 11.2 |
| 2Al_CAM(+T) Initial | 39 | 51 | 10 |
| 2Al_CAM(+T) Final | 44.4 | 43.7 | 11.9 |
| 2Al_CA Initial | 43 | 57 | 0 |
| 2Al_CA Final | 42.0 | 47.3 | 10.7 |

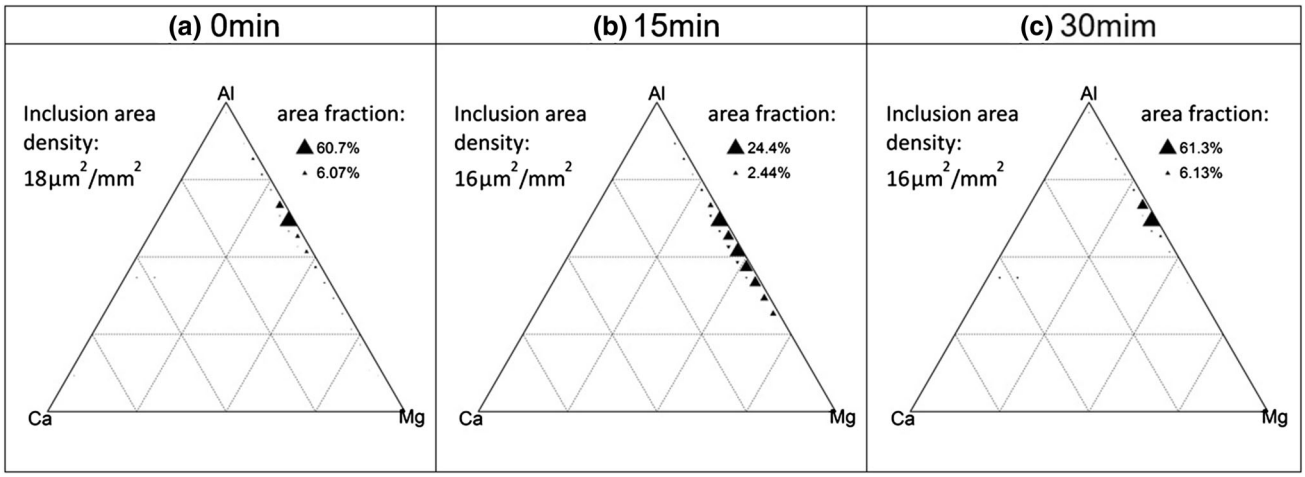


Fig. 4—Evolution of inclusion chemistry with time—(*a*) 0 min, (*b*) 15 min, (*c*) 30 min—for experiment 2AL_NONE. The 0-min sample was taken 30 min after melting. This homogenization hold was conducted for all experiments, after which slag was added in the experiments reported below. These samples were labeled this way so that they could be compared to the experiments with slag additions.

in Figure 8. The inclusions were modified to MgO with variable Ca/Al contents. As in the experiments at 1873 K (1600 °C), more Ca modification occurred at higher Al levels.

## IV. DISCUSSION

In the experimental results reported above, inclusion evolution was studied in Fe-Al melts with Al contents varying from 0.1 to 2 wt pct. Initially $Al_2O_3$ inclusions were modified by Mg and Ca from the slag and the crucible. Without slag, the inclusions transformed from $Al_2O_3 \rightarrow$ Spinel. With slag, the sequence of inclusion chemistry changes was $Al_2O_3 \rightarrow$ Spinel $\rightarrow$ MgO $\rightarrow$ MgO + CaO-$Al_2O_3$-MgO. This sequence was similar regardless of whether MgO was added to the initial slag. The rate of Mg and Ca transfer increased with increasing Al level. It was also found that increased temperature increased the rate of inclusion modification.

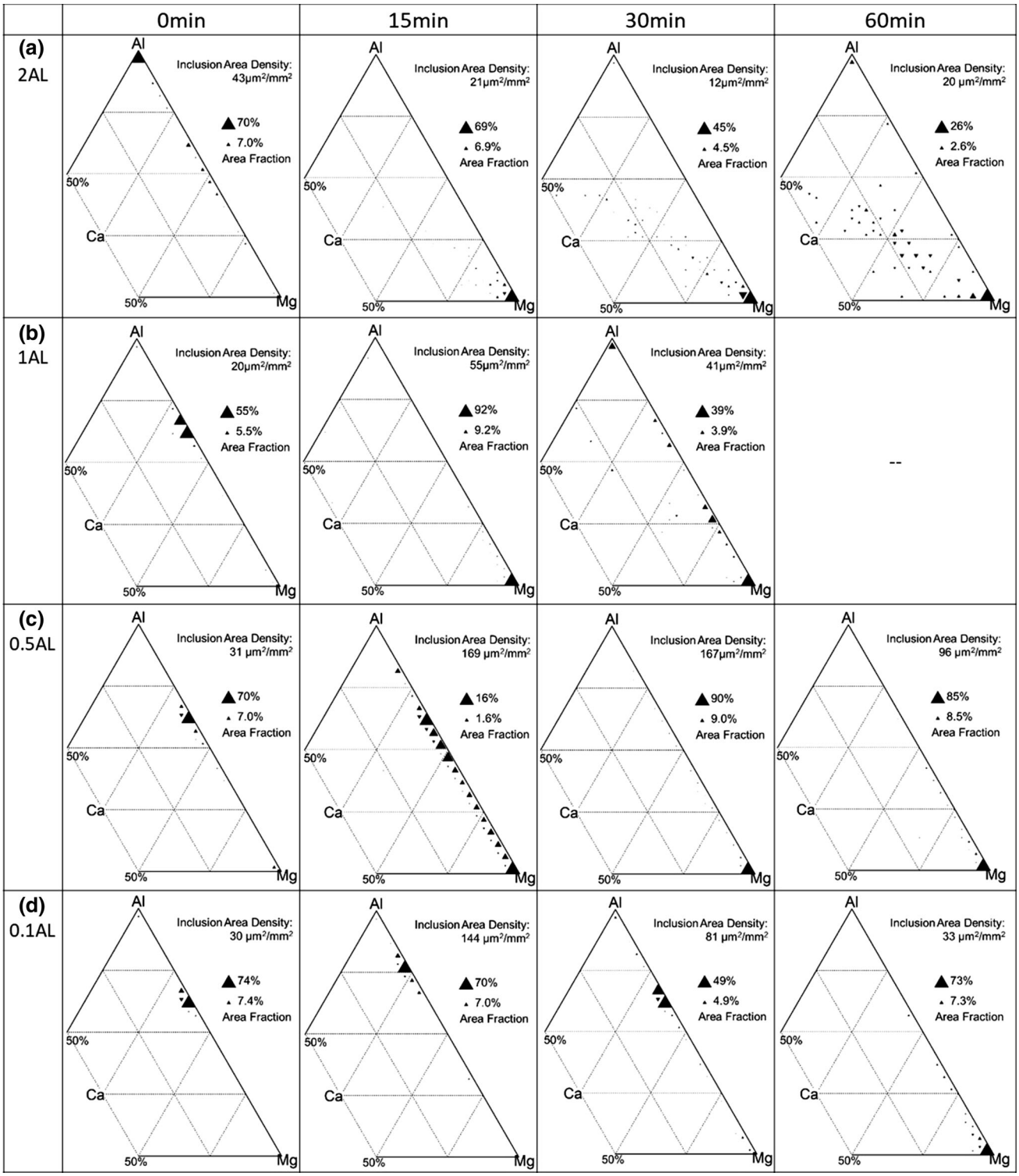


Fig. 5—Evolution of inclusion chemistry with time in experiments with the CAM slag (*a*) 2AL_CAM, (*b*) 1AL_CAM, (*c*) 0.5AL_CAM, and (*d*) 0.1AL_CAM.

The modification of inclusions occurs by supply reactions at the slag/metal (or crucible/metal) interface and consumption reactions at the metal/inclusion interface. The two reactions are connected by dissolved species in the metal. The Ca and Mg supply reactions are

$$2[\mathrm{Al}]_{\mathrm{metal}} + 3(\mathrm{MgO})_{\mathrm{slag}} = 3[\mathrm{Mg}]_{\mathrm{metal}} + (\mathrm{Al_2O_3})_{\mathrm{slag}}, \quad [1]$$

$$2[\mathrm{Al}]_{\mathrm{metal}} + 3(\mathrm{CaO})_{\mathrm{slag}} = 3[\mathrm{Ca}]_{\mathrm{metal}} + (\mathrm{Al_2O_3})_{\mathrm{slag}}. \quad [2]$$

Mg was also supplied from the crucible *via* reaction [3]

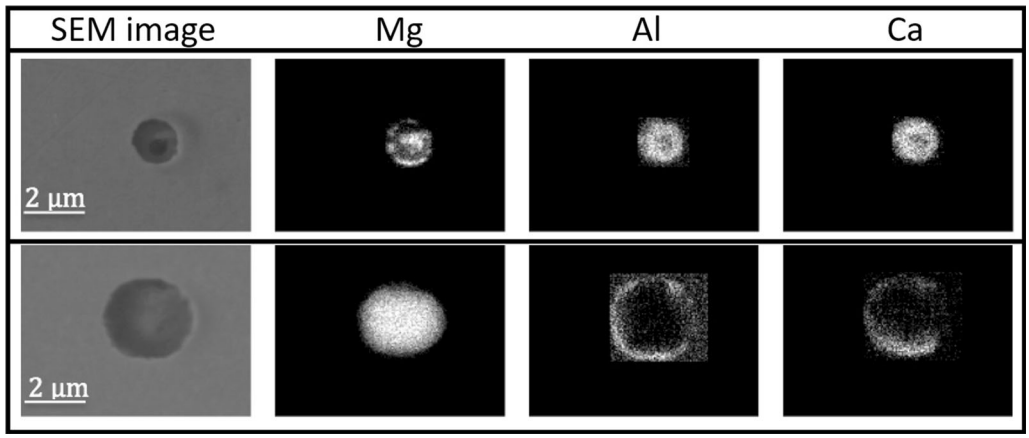


Fig. 6—EDS mapping showing spatial distribution of Mg, Al, and Ca in two Ca-containing inclusions from 30 min 2AL_CAM sample.

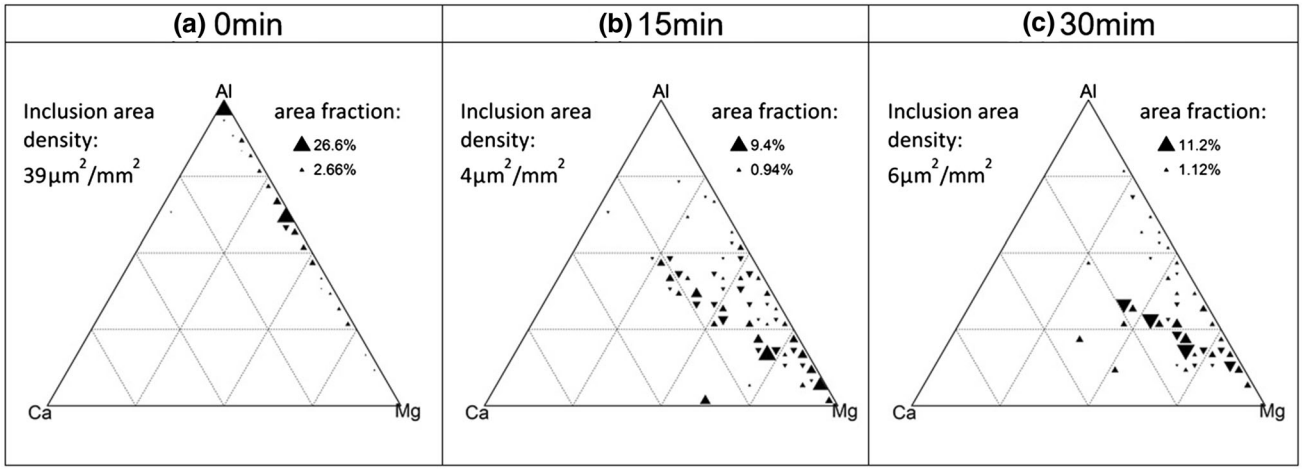


Fig. 7—Evolution of inclusion chemistry with time—(*a*) 0 min, (*b*) 15 min, (*c*) 30 min—for experiment 2AL_CA.

$$2[\mathrm{Al}]_{\mathrm{metal}} + 3(\mathrm{MgO})_{\mathrm{crucible}} = 3[\mathrm{Mg}]_{\mathrm{metal}} + (\mathrm{Al_2O_3})_{\mathrm{crucible}}. \quad [3]$$

The contribution of Mg from reaction [3] relative to that from slag was expected to be low. Since the crucible is solid, the rate-controlling process for reaction [3] was likely solid-state diffusion of $Al_2O_3$ away from the metal/crucible interface. This means the overall rate of Mg supplied to the melt would be slower than the liquid phase mass transfer-controlled reaction [1]. This was consistent with experimental results—Mg modification in 2AL_NONE (Figure 4) was slower and spinel inclusions were observed compared to MgO inclusion formation in 2AL_CAM (Figure 5(a)). It was also possible that Mg vaporized from the exposed steel surface.[34] The inclusion composition would be determined by the balance of supply and removal due to vaporization.

The consumption of Mg and Ca at the inclusions occurred *via* several different reactions. To form spinels, from the initial $Al_2O_3$, the following reaction occurred:

$$3[\mathrm{Mg}]_{\mathrm{metal}} + 4(\mathrm{Al_2O_3})_{\mathrm{inclusion}} = 3(\mathrm{MgO}\cdot\mathrm{Al_2O_3})_{\mathrm{inclusion}} + 2[\mathrm{Al}]_{\mathrm{metal}}. \quad [4]$$

To form MgO inclusions from the spinels, the following reaction occurred:

$$3[\mathrm{Mg}]_{\mathrm{metal}} + (\mathrm{MgO}\cdot\mathrm{Al_2O_3})_{\mathrm{inclusion}} = 4(\mathrm{MgO})_{\mathrm{inclusion}} + 2[\mathrm{Al}]_{\mathrm{metal}}. \quad [5]$$

The stability of MgO can be confirmed by writing the overall reaction for MgO formation, the sum of reactions [5] and [1]

$$3(\mathrm{MgO})_{\mathrm{slag}} + (\mathrm{MgO}\cdot\mathrm{Al_2O_3})_{\mathrm{inclusion}} = 4(\mathrm{MgO})_{\mathrm{inclusion}} + (\mathrm{Al_2O_3})_{\mathrm{slag}}. \quad [6]$$

The equilibrium constant of reaction [6] is the same as that for spinel decomposition:

$$(\mathrm{MgO}\cdot\mathrm{Al_2O_3})_{\mathrm{inclusion}} = (\mathrm{MgO})_{\mathrm{inclusion}} + (\mathrm{Al_2O_3})_{\mathrm{slag}}. \quad [7]$$

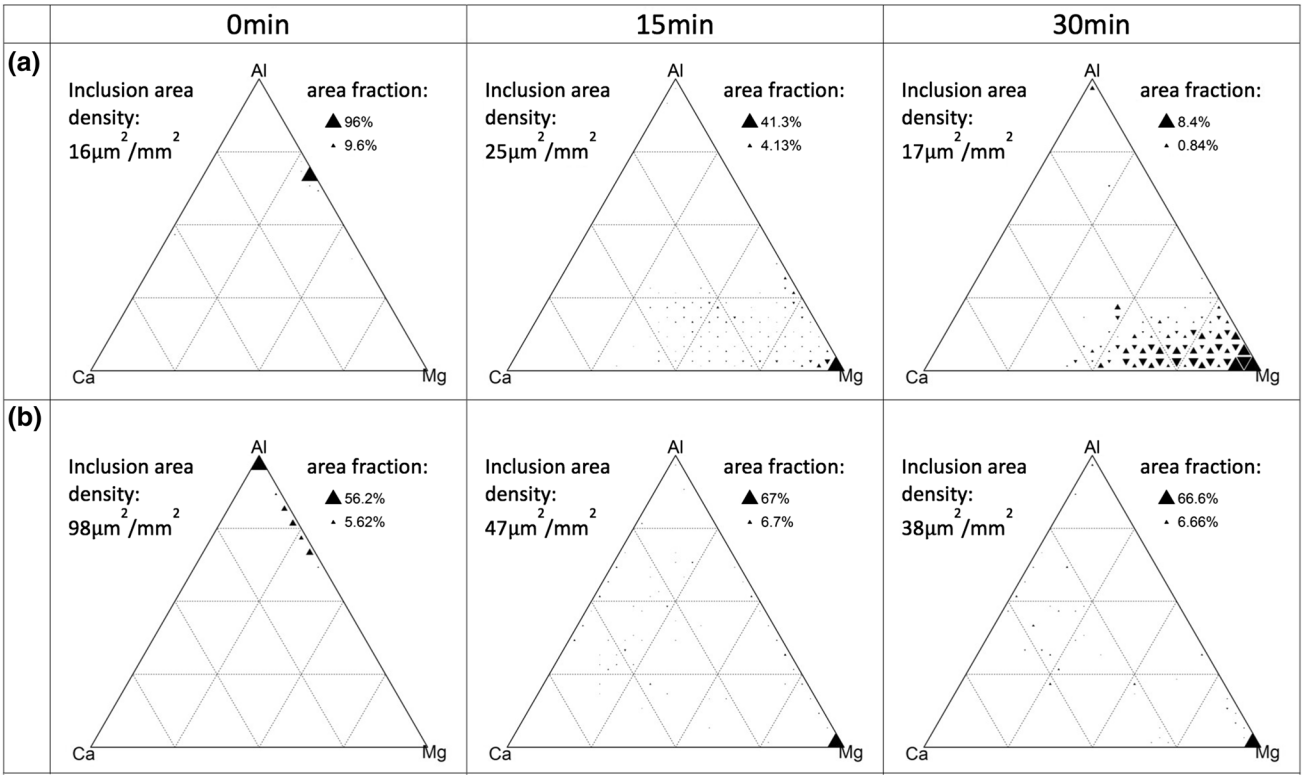


Fig. 8—The evolution of inclusion chemistry with time for (*a*) 2AL_CAM (+T) and (*b*) 1AL_CAM (+T).

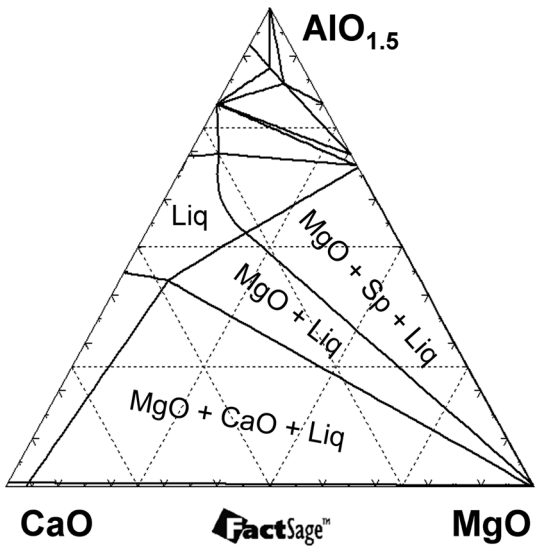


Fig. 9—Isothermal section of the AlO1.5-CaO-MgO system at 1873 K (1600 °C), P = 1 atm. The simulation included CaO and MgO as solution phases to show the limited solubility of Ca and Al in MgO.

**Table IV. Average Diameter of Inclusions after 60 min in Experiments 2AL_CAM and 2AL_CA**

| | 2AL_CAM ($\mu$m) | 2AL_CA ($\mu$m) |
|---|---|---|
| Mg Mole Fraction > 0.8 | 1.37 | 1.64 |
| Mg Mole Fraction < 0.8 | 1.10 | 0.82 |

The equilibrium constant for this reaction is 0.097 at 1873 K (1600 °C) per FactSage. A value of 0.04 would be calculated from the data of Fujii.[35] The reaction quotient for this reaction is

$$Q = \frac{a_{Al_2O_3(slag)} a_{MgO(inclusion)}}{a_{(MgO \cdot Al_2O_3)_{inclusion}}} = \frac{(0.006)(1)}{0.8} = 0.0075. \quad [8]$$

The $Al_2O_3$ activity (relative to pure solid oxide) was calculated for the slag composition in this study using FactSage. The low value of 0.006 was consistent with measured $Al_2O_3$ activities in the ternary slag system[36] with pure solid oxides as the standard state. The spinel activity was taken assuming MgO-saturated spinels[35] with stoichiometric spinels as the standard state. Since there was a thermodynamic driving force for this reaction to proceed and MgO inclusions are thermodynamically stable. This was a consequence of the CaO, MgO-saturated slags with low $Al_2O_3$ activity used in this work. The observed inclusion evolution results were consistent with previous studies using high-basicity slags.[9,37] Initially omitting MgO from the slag did not have a large effect on the inclusion evolution. The inclusions from experiment 2AL_CA (Figure 7) evolved similarly to the inclusions in 2AL_CAM and the dissolution of MgO from the crucible to the slag was not considered to be rate determining. The slags were MgO-saturated by the end of the experiment as shown in Table III.

The Ca in inclusions was supplied by reaction [2], but the amount of Ca in the inclusions was much lower than Mg. The specific reactions of Ca with inclusions depended on the inclusion Mg content. Assuming liquid

Table V. Equilibrium Mg and Ca (Calculated by FactSage) in Liquid Fe for Fe-Al Alloys in Equilibrium with a 51 Wt Pct CaO, 39 Wt Pct $Al_2O_3$, 10 Wt Pct MgO Slag

| $T$ | Al (Weight Percent) | FactSage [ppm] | Max Measured [ppm] | FactSage [ppm] |
|---|---|---|---|---|
| 1873 K (1600 °C) | 2 | 114 | 72 | 13 |
| | 1 | 58 | — | 13 |
| | 0.5 | 35 | 35 | 12 |
| | 0.1 | 16 | — | 12 |
| 1973 K (1700 °C) | 2 | 363 | 172 | 62 |
| | 1 | 196 | 87 | 60 |

For Measured [Mg] values, the amount of Mg in the inclusions was subtracted. Measured [Ca] values were reported to be less than 10 ppm, but there was high uncertainty so individual measurements were not reported.

inclusions form (consistent with experimental results), then the following reactions can be written as follows:

If the inclusion Mg content was essentially zero,

$$3[Ca]_{metal} + (3x+1)(Al_2O_3)_{inclusion} = 3(CaO \cdot xAl_2O_3)_{inclusion} + 2[Al]_{metal}. \quad [9]$$

If the inclusions were spinels,

$$[Ca]_{metal} + (MgO \cdot yAl_2O_3)_{inclusion} = (CaO \cdot yAl_2O_3)_{inclusion} + [Mg]_{metal}. \quad [10]$$

If the inclusions were MgO,

$$[Ca]_{metal} + 2z[Al]_{metal} + (3z+1)(MgO)_{inclusion} = (CaO \cdot zAl_2O_3)_{inclusion} + (3z+1)[Mg]_{metal}. \quad [11]$$

There will be some dissolved MgO in the liquid calcium aluminates that is not represented in the above reactions. Figure 6 showed examples of reaction [11]—inclusions with MgO cores and liquid calcium aluminate (with a small amount of dissolved MgO) shells.

The sequence of inclusion modification $Al_2O_3 \rightarrow$ Spinel $\rightarrow$ MgO $\rightarrow$ MgO + CaO-$Al_2O_3$-MgO has been reported in other work on inclusion evolution in Al-deoxidized melts.[9,10,37,38] Spinel inclusions were observed by Okuyama[10] when the steel contained 0.1 wt pct Al and the slag chemistry was 57 wt pct CaO, 5 wt pct $SiO_2$, 28 wt pct $Al_2O_3$, and 10 wt pct MgO. In this prior study, spinel inclusions formed after 15 minutes reaction, but inclusion compositions were not reported for longer times. No Ca-containing inclusions were reported. In the current study, MgO inclusions with very low Ca levels formed, even at 0.1 wt pct Al. The difference could be attributed to the longer hold time or because the experiments of Okuyama contained $SiO_2$,[38] reduction of which would consume some Al. The observation of MgO-rich inclusions was consistent with studies from both Todoroki and Jiang.[9,37] In these studies, even longer times were employed (up to 180 minutes), after which fully liquid CaO-MgO-$Al_2O_3$ inclusions were observed.

Fully liquid inclusions were not observed in this work. It was possible that equilibrium was not fully attained in the times examined. However, in equilibrium only the component activities must be equal, not compositions. Figure 9 shows the $AlO_{1.5}$-CaO-MgO phase diagram at 1873 K (1600 °C) (generated from FactSage). It should be possible for an inclusion to be MgO-rich in composition and still be in equilibrium with a CaO-, MgO-saturated liquid slag.

The occurrence of predominately liquid inclusions in previous studies might be attributed to inclusion size and flotation. Consumption of Ca and Al at smaller inclusions might be locally faster and so smaller inclusions would have more Ca,Al-rich liquid. The larger, MgO-rich inclusions would then mostly have floated out after 180 minutes. There was some supporting evidence of this from the inclusion sizes in experiments 2AL_CAM and 2AL_CA. Table IV shows that after 60 minutes, in samples of both experiments, MgO-rich inclusions (Mg mole fraction $> 0.8$) had an average diameter larger than inclusions with Mg mole fraction $< 0.8$. Further analysis on inclusion chemistry trajectories and potential size effects will be reported in the future.

In samples taken from production processes, predominately liquid inclusions were often observed.[8,20] In studies such as these stirring will strongly affect slag/metal mass transfer as well as inclusion flotation. Therefore, deviations between gas-stirred ladles and the laboratory-scale studies would be expected.

The reactions above proceed by mass transport of Mg and Ca at the slag/metal interface and at the metal/inclusion interface. Calculations by Okuyama suggested that mass transfer of Mg in the metal at the slag/metal interface controlled the rate of spinel formation in lab-scale experiments.[10] Recently Wang *et al.* identified mass transfer of Ca at the slag/metal interface as determining the rate of inclusion modification by Ca.[39] In the current study, there was an apparent effect of metal Al content on mass transfer, with faster Mg and Ca modification occurring at higher Al levels. Modification was also faster at higher temperature. Assuming the rate-controlling step was mass transfer at the slag/metal interface, then this observation could be attributed to the effect of Al and temperature on the mass transfer driving force, which was related to the equilibrium dissolved [Mg] and [Ca] levels at the slag/metal interface. These values were calculated *via* FactSage and are presented in Table V. The table also presents a comparison to measured values for Mg levels.

The equilibrium [Mg] values were generally higher than those for [Ca], which was consistent with the observation of faster Mg modification at higher Al. The equilibrium [Mg] values increased with increasing [Al], while the [Ca] values did not. The predicted values increased significantly with temperature, which was consistent with experimental observations of faster Mg and Ca modification at elevated temperature.

There were several factors that led to the deviations between the predicted and the maximum measured values. First, reoxidation was evident in several samples. This would lower dissolved Al levels by an amount that depended on the extent of reoxidation. The lower dissolved Al would result in lower mass transfer driving force. However, the trend of higher expected driving force with higher [Al] levels was still consistent with the calculations. The elevated temperature experiment was not held at 1973 K (1700 °C); actual temperatures were lower and somewhat variable. Given the temperature sensitivity, lower measured values were expected. These results do suggest though that local conditions, *e.g.*, nearer the arc during reheating in the ladle, might significantly change the Mg and Ca reaction kinetics on the industrial scale.

## V. CONCLUSIONS

CaO and MgO reduction by Al in liquid steel and subsequent inclusion changes were simulated in laboratory experiments. Experiments were conducted to evaluate the effects of Al content in steel and reaction temperature. The following conclusions were obtained:

1. Dissolved Al reduced MgO and CaO from the slag and from the crucible, leading to Mg and Ca modification of inclusions.
2. The path of inclusion composition evolution was $Al_2O_3 \rightarrow$ Spinel $\rightarrow$ MgO $\rightarrow$ MgO + CaO-$Al_2O_3$-MgO. Possible reactions that led to this sequence have been described.
3. Mg modification occurred faster than Ca modification. Both were faster at elevated Al levels and at elevated temperature. This was attributed to differences in the driving force for mass transfer at the slag/metal interface.

## ACKNOWLEDGMENTS

We gratefully acknowledge support from the industrial members of the Center for Iron and Steelmaking Research as well as helpful discussions with Prof. Chris Pistorius. We also acknowledge the use of the Materials Characterization Facility at Carnegie Mellon University supported by Grant MCF-677785.

## REFERENCES

1. R. Kuziak, R. Kawalla, and S. Waengler: *Arch. Civil Mech. Eng.*, 2008, vol. 8, pp. 103–17.
2. Advanced high strength steel (AHSS) application guidelines, Version 5.0, May 2014, www.worldautosteel.org.
3. H. Qu, G.M. Michal, and A.H. Heuer: *Metall. Mater. Trans. A*, 2013, vol. 44A, pp. 4450–53.
4. J.H. Park, S.B. Lee, and D.S. Kim: *Metall. Mater. Trans. B*, 2005, vol. 36B, pp. 67–73.
5. H. Itoh, M. Hino, and S. Ban-Ya: *Metall. Mater. Trans. B*, 1997, vol. 28B, pp. 953–56.
6. J.H. Park and H. Todoroki: *ISIJ Int.*, 2010, vol. 50, pp. 1333–46.
7. K. YoungJo, L. Fan, M. Kazuki, and S. Du: *Steel Res. Int.*, 2006, vol. 77, pp. 785–92.
8. Z. Deng and M. Zhu: *ISIJ Int.*, 2013, vol. 53, pp. 450–58.
9. H. Todoroki and K. Mizuno: *Iron Steelmak.*, 2003, vol. 30, pp. 60–67.
10. G. Okuyama, K. Yamaguchi, S. Takeuchi, and K.I. Sorimachi: *ISIJ Int.*, 2000, vol. 40, pp. 121–28.
11. A. Harada, G. Miyano, N. Maruoka, H. Shibata, and S.Y. Kitamura: *ISIJ Int.*, 2014, vol. 54, pp. 2230–38.
12. A. Harada, N. Maruoka, H. Shibata, and S.Y. Kitamura: *ISIJ Int.*, 2013, vol. 53, pp. 2110–17.
13. A. Harada, N. Maruoka, H. Shibata, and S.Y. Kitamura: *ISIJ Int.*, 2013, vol. 53, pp. 2118–25.
14. T. Yoshioka, K. Nakahata, T. Kawamura, and Y. Ohba: *ISIJ Int.*, 2016, vol. 56, pp. 1973–81.
15. W. Yang, L. Zhang, and X. Wang: *ISIJ Int.*, 2013, vol. 53, pp. 1401–10.
16. E.B. Pretorius, H.G. Oltmann, and T. Cash: *Iron Steel Technol.*, 2010, vol. 7, pp. 31–44.
17. N. Verma, M. Lind, P.C. Pistorius, R.J. Fruehan, and M. Potter: *Iron Steel Technol.*, 2010, vol. 7, pp. 189–97.
18. T. Zhang, Y. Min, C. Liu, and M. Jiang: *ISIJ Int.*, 2015, vol. 55, pp. 1541–48.
19. I.H. Jung, S.A. Decterov, and A.D. Pelton: *Metall. Mater.Trans. B*, 2004, vol. 35, pp. 493–507.
20. E.B. Pretorius, H.G. Oltmann, and B.T. Schart: *Proc. AISTech 2013 Iron Steel Technol. Conf. Expos.*, Pittsburgh, PA, 2013, vol. II, pp. 993–1026.
21. S.R. Story and R.I. Asfahani: *Proc. AISTech 2013 Iron Steel Technol. Conf. Expos.*, Pittsburgh, PA, 2013, vol. II, pp. 1201–13.
22. P. Kaushik and H. Yin: *AIST Trans.*, 2012, vol. 9, pp. 165–83.
23. D.J. Kim and J.H. Park: *Metall. Mater. Trans. B*, 2012, vol. 43B, pp. 875–86.
24. W.K. Lewis and W.G. Whitman: *Ind. Eng. Chem.*, 1924, vol. 16, pp. 1215–20.
25. R. Higbie: *Trans. AIChE.*, 1935, vol. 31, pp. 365–89.
26. J.H. Shin, Y. Chung, and J.H. Park: *Metall. Mater. Trans. B*, 2017, vol. 48B, pp. 46–59.
27. S.P. Piva, D. Kumar, and P.C. Pistorius: *Metall. Mater. Trans. B*, 2017, vol. 48B, pp. 37–45.
28. M. Arnulf and E.F. Osborn: *Phase Equilibrium among Oxides in Steelmaking*, Addison Wesley Publishing Company, Reading, MA, 1965.
29. Y. Ren, Y. Zhang, and L. Zhang: *Ironmak. Steelmak.*, 2017, vol. 44, pp. 497–504.
30. H. Ohta and H. Suito: *ISIJ Int.*, 1996, vol. 36, pp. 983–90.
31. M.A. Tayeb, A.N. Assis, S. Sridhar, and R.J. Fruehan: *Metall. Mater. Trans. B*, 2015, vol. 46B, pp. 1112–14.
32. P.C. Pistorius and N. Verma: *Microsc. Microanal.*, 2011, vol. 17, pp. 963–71.
33. C.W. Bale, P. Chartrand, S.A. Degterov, G. Eriksson, K. Hack, R.B. Mahfoud, J. Melançon, A.D. Pelton, and S. Petersen: *Calphad*, 2002, vol. 26, pp. 189–228.
34. H. Mu, T. Zhang, L. Yang, R.R. Xavier, R. Fruehan, and B.A. Webler: *Metall. Mater. Trans. B*, 2016, vol. 47B, pp. 3375–83.
35. K. Fujii, T. Nagasaka, and M. Hino: *ISIJ Int.*, 2000, vol. 40, pp. 1059–66.
36. R. Inoue and H. Suito: *Metall. Mater. Trans. B*, 1994, vol. 25B, pp. 235–44.
37. M. Jiang, X. Wang, B. Chen, and W. Wang: *ISIJ Int.*, 2010, vol. 50, pp. 95–104.
38. H. Todoroki and K. Mizuno: *ISIJ Int.*, 2004, vol. 44, pp. 1350–57.
39. Q. Wang, L. Wang, J. Zhai, J. Li, and K.C. Chou: *Metall. Mater. Trans. B*, 2017, vol. 48B, pp. 564–72.